Pharm Res (2015) 32:61–73
DOI 10.1007/s11095-014-1444-x

RESEARCH PAPER

Prevention of Biofilm Formation by Methacrylate-Based Copolymer Films Loaded With Rifampin, Clarithromycin, Doxycycline Alone or in Combination

Warren E. Rose • Daniel P. Otto • Marique E. Aucamp • Zach Miller • Melgardt M. de Villiers

Received: 7 April 2014 / Accepted: 10 June 2014 / Published online: 17 June 2014

ABSTRACT

Purpose This study reports the incorporation of the antibiotics rifampin, doxycycline and clarithromycin in poly(styrene-*co*-methyl methacrylate films and their effect on biofilm prevention.

Background Invasive procedures in patients such as surgical device, or intravenous or urinary catheter implantation, often results in complicated hospital-acquired nosocomial infections. Biofilm formation is essential to establish these infections on these devices and novel antibiotic delivery approaches are needed for more effective management.

Methods The films were evaluated *in vitro* for drug release and for their ability to prevent biofilm formation by methicillin susceptible and methicillin resistant *Staphylococcus aureus*. Surface tension components, obtained from contact angle measurements, and the morphology of the films evaluated by scanning electron microscopy were also investigated.

Results In this study, antibiotic-loaded methacrylic copolymer films that effectively released rifampin, clarithromycin and doxycycline for up to 21 days prevented biofilm formation when tested in an *in vitro* bioreactor model. These drug loaded copolymer films provided the advantage by coating materials with a novel surface that was unsuitable for resettling of biofilms once the antibiotic was dissolved from the polymer surface. A combination of rifampin and clarithromycin released from the polymer film provided >99.9% kill of an MRSA inoculate for up to 72 h.

Conclusion Results showed that combining multiple drugs in copolymer films with unique surface properties, initial hydrophilicity and increase in roughness, can be an effective way to prevent biofilm formation.

KEY WORDS antibiotic · biofilm · drip flow bioreactor · methacrylate copolymer coating

ABBREVIATIONS

CLR	Clarithromycin
DIM	Diiodomethane
DOX	Doxycycline
EG	Ethylene glycol
GPC-MALLS-RI	Gel permeation chromatography coupled to multi-angle laser light scattering and refractive index double detection
HQ	Hydroquinone
KPS	Potassium persulphate
MMA	Methyl methacrylate
MRSA	Methicillin-resistant *Staphylococcus aureus*
MSSA	Methicillin-susceptible *Staphylococcus aureus*
Poly(S-*co*-MMA)	Poly(styrene-*co*-methyl methacrylate)
RIF	Rifampicin
S	Styrene
SDS	Sodium dodecyl sulphate
W_A	Work of adhesion

INTRODUCTION

A continuously growing need to curb hospital-acquired infections has resulted in the recognition of microbial biofilms as a pivotal cause of persistent infections (1). Some of the most

Electronic supplementary material The online version of this article (doi:10.1007/s11095-014-1444-x) contains supplementary material, which is available to authorized users.

W. E. Rose • Z. Miller • M. M. de Villiers (✉)
School of Pharmacy, University of Wisconsin
777 Highland Avenue, Madison, Wisconsin 53705-2222, USA
e-mail: mmdevilliers@pharmacy.wisc.edu

D. P. Otto
Research Focus Area for Chemical Resource Beneficiation
Catalysis and Synthesis Research Group, North-West University
Potchefstroom, South Africa

M. E. Aucamp
Centre of Excellence for Pharmaceutical Sciences
North-West University, Potchefstroom, South Africa

commonly hospital-acquired infections on devices are attributed to methicillin-resistant *Staphylococcus aureus* (MRSA) and *Pseudomonas aeruginosa* (2).

The difficulty in treating these infections is, amongst others, attributed to formation of a therapy-resistant biofilm comprising these microorganisms (3). A typical example is the reduction in diffusion of gentamicin and tobramycin into *P. aeruginosa* biofilms (4). The resistance of biofilms to chemotherapy arises from the structural composition of a biofilm. Although variable between various organisms, the biofilm comprises approximately 85% of a biomatrix, which contains secreted proteins, DNA and polysaccharides to produce a significant permeation barrier to drugs. Only a small portion of the biofilm (15%) contains microorganisms (5). Microorganisms that mature in the biofilm can also actively secrete agents that further suppress the immune system of the host (6).

When biofilms form after implantation of medical devices, it carries the risk of device-related infection and can result in the patient suffering worse health after treatment than before receiving medical care (7). Common medical devices that can host biofilms are indwelling catheters (8), orthopedic prosthetic implants (9) and surgical equipment (7). Although the incidence of device-related infections has remained consistently low, significantly more patients undergo these procedures and therefore, a greater number of these infections are expected. Several strategies have been developed to modify surfaces of objects in order to prevent or exterminate biofilms. These include surface modification of metal oxides such as coating with silver particles, coating of surfaces with disinfectants such as silver sulfadiazine and direct contact killing of microorganisms with (poly)cations for example trimethylated chitosan (10–12).

The polymer surface roughness can also alter biofilm adhesion to a surface as illustrated for *E. coli* biofilms (13). Lastly, another structural property that influences adhesion of microorganism to polymeric films is the elasticity of the membrane (14).

In this study, various antibiotics and their combinations, which were loaded into methacrylate-based copolymeric films that exhibit differences in structural and surface properties, is reported. The combined effect of the drugs and surface properties seem to be very effective at curbing the establishment and growth of biofilms formed by methicillin-susceptible (MSSA) and methicillin-resistant (MRSA) *S. aureus*.

MATERIALS AND METHODS

Materials

Reagent grade THF, *n*-butanol (BuOH), styrene (S), potassium persulfate (KPS), hydroquinone (HQ), sodium dodecyl sulfate (SDS) and basic alumina were purchased from Sigma Aldrich (Kempton Park, South Africa). Methyl methacrylate (MMA) was donated by Evonik Industries (Johannesburg, South Africa). Double deionized water was used in the emulsion copolymerization reactions to prepare the dispersion medium. Rifampin (RIF), clarithromycin (CLR) and doxycycline (DOX) were received as donations (Toku-E, Bellingham, WA, USA). Reagent grade diiodomethane (DIM) and ethylene glycol (EG) were obtained from Sigma-Aldrich (Milwaukee, WI). The surface tension properties of DIM, EG and water are listed in Table I.

Copolymerization

Detailed outlines of the polymerization procedure used to prepare the poly(styrene-*co*-methacrylate) polymers were previously reported by us (15). Briefly, suitable quantities of the monomers were passed through an alumina column to remove the inhibitors and transferred to the reaction vessel and emulsified in the dispersion medium. The dispersion medium contained deionized water, SDS and BuOH. KPS was dissolved in the appropriate volume of deionized water and heated to the appropriate temperature before it was injected to the temperature-controlled reaction medium. The reaction vessel was maintained at the required temperature for 2 h and the polymer recovered by precipitation in methanol with addition of HQ to quench the reaction. The precipitated copolymer was dissolved in THF and passed through an alumina column for purification. The purified copolymeric product was characterized as we described earlier and GPC-MALLS-RI was used to determine weight average molecular weight, $\overline{M}_w$ and number average molecular weight, $\overline{M}_n$ and the polydispersity index which is the ratio of these values (15).

Film Casting

The copolymers that were selected were designated as M9, M28, M44 and their properties are listed in Table II. A suitable quantity of the copolymers was dispersed by sonication in THF to produce 5% (w/v) latex of the polymer and dissolved over a period of 24 h. The antibiotics were dissolved in THF and added to the polymer latex as single drugs or drug combinations. For films containing pure antibiotic or combinations of antibiotics no addition to the polymer latex was performed. Solvent casting was used to produce films on the surface of a microscope slide ($n=6$). A volume of approximately 7 mL was cast onto a cleaned, weighed microscope slide (7.6×2.5 cm) and left to dry at 23°C for 12 h, followed by additional drying at 40°C to constant weight (16). The slide was weighed with the copolymer coat still attached to the slide and the deposited weight calculated. Films were cast from pure polymers M9, M28 and M44 as well as 1:1 w/w mixtures of M28:M49 and M28:M9 as controls and with pure

Table I Surface tension components, γ, and parameters of the probe liquids mostly used to determine contributions of polar and apolar interactions between phases. Unit of γ is given in mJ/m^2 (21)

Probe	γ	γ^{LW}	γ^{AB}	γ^+	γ^-
DIM	50.8	50.8	0	0	0
Water	72.8	21.8	51.0	25.5	25.5
EG	48	29	19	1.92	47

antibiotics or 1:1 w/w combinations of RIF:DOX or RIF:CLR. Films were wrapped in aluminum foil and stored in a closed container until use.

Drug Release

A strip of copolymer film was cut to fit inside a basket as specified by the USP basket dissolution method (17). The release was performed at pH 7.40 in phosphate buffered saline (PBS) solution at 37°C (n=6). The rotational speed of the baskets was set to 50 rpm and dissolution vessels were filled with 500 mL dissolution medium. The release vessel was sampled at regular intervals by withdrawal of 5 mL aliquots followed by immediate replenishment of the release vessel with PBS. The drug release from films containing single drugs was monitored UV-spectrophotometrically at 475 nm for RIF and 268 nm for DOX (17). The HPLC methods described in the USP for assay and dissolution testing were used to monitor CLR release and drug release from films containing combination drugs (17, 18). In a separate experiment drug-coated slides (n=4) were placed in the bioreactor and at predetermined times samples were taken from the effluent and analyzed for drug content using the HPLC methods.

Scanning Electron Microscopy

Various film samples were evaluated using scanning electron microscopy (SEM). Samples were taken before, during and after release experiments and bioreactor studies. Samples were mounted on double-sided carbon tape stubs and coated with Au/Pd under vacuum in an argon atmosphere. Images were recorded with a Hitachi S570 electron microscope at a 10 keV crystal source emission.

Table II Properties of the synthesized copolymers. Molecular weight in 1×10^4 g/mol

Copolymer	$\overline{M}_n$	$\overline{M}_w$	$\overline{M}_w/\overline{M}_n$	%MMA	%S
M9	8.41	15.1	1.96	31.8	68.2
M28	23.5	41.2	1.76	33.3	66.7
M44	8.27	15.9	1.81	29.7	70.3

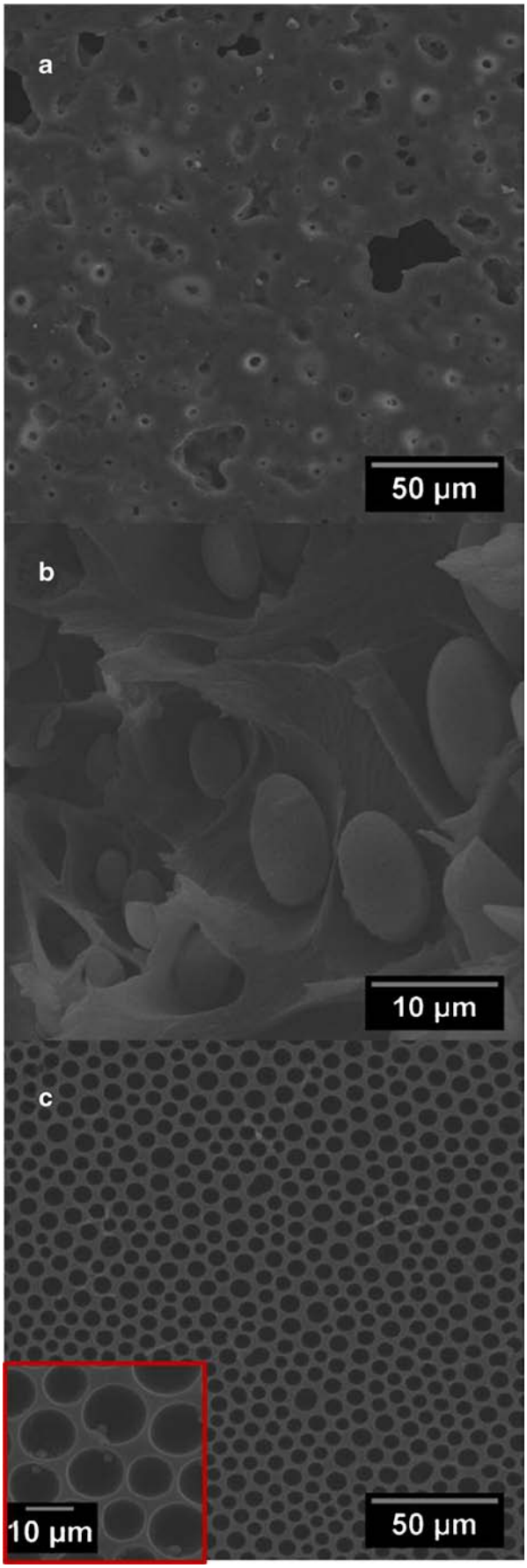

◀ **Fig. 1** SEM image of a ~400 μm-thick film which was loaded to contain 10% w/w RIF. (**a**) shows the surface pores opening after erosion of drug from the surface within a period of 4 h. (**b**) shows the interior honeycomb structure of the film with some drug particle remaining in the pockets whilst others have partially dissolved. (**c**) (and inset) shows the empty surface cavities of the film after 72 h of exposure to the release medium.

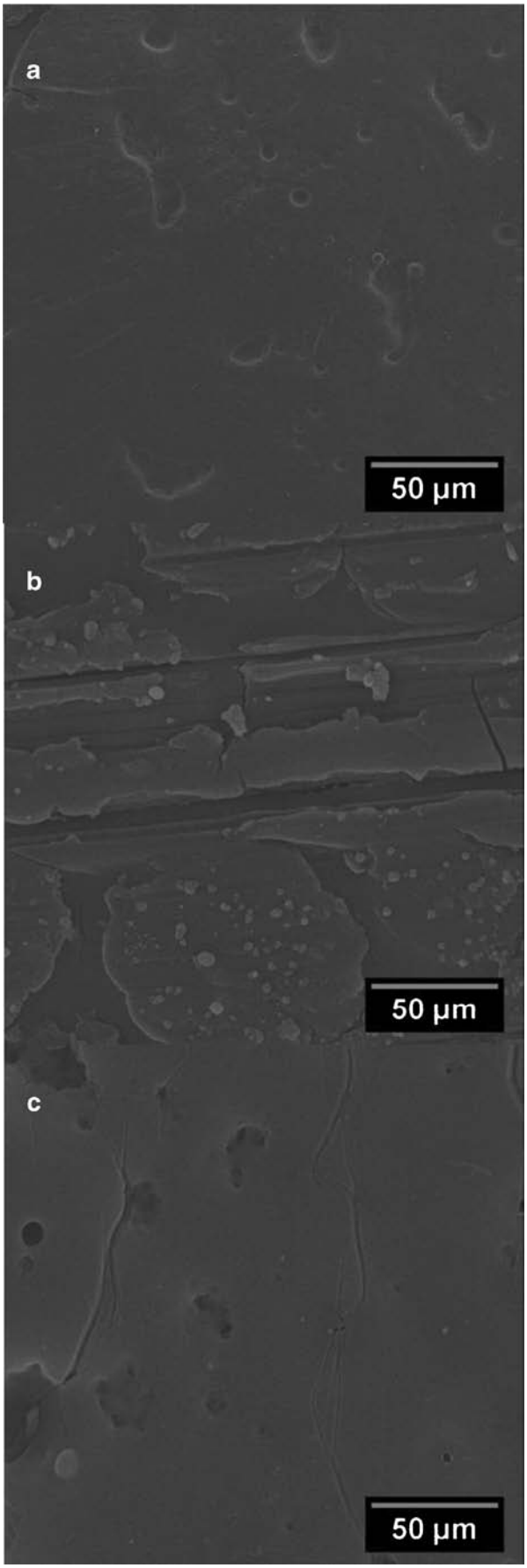

Contact Angles and Free Surface Energy Calculations

The contact angle and surface tension of a pure liquid, pure solid and pure vapor was first related by the Young equation (19). A modified Young equation, the expanded Young-Dupré equation, can be applied to determine the work of adhesion for solid–liquid contact for contact angles between 0 and 180° (20). (See supplementary information) In this equation the apolar component of the surface tension or Lifshitz-van der Waals-components are developed and related to the contact angle measured between different components, such as a solid–liquid interface:

$$(1+cos\theta)\gamma_L = 2\left[\left(\gamma_S^{LW}\gamma_L^{LW}\right)^{1/2} + \left(\gamma_S^{+}\gamma_L^{-}\right)^{1/2} + \left(\gamma_S^{-}\gamma_L^{+}\right)^{1/2}\right] \quad (1)$$

To ensure that all the different components that contribute to the interfacial tension are accounted for, at least 3 liquids, with different polarities must be used for contact angle measurements and substituted in Eq. 4 for surface tension component evaluation. As a prerequisite, 2 of the liquids should be polar, however fall in different categories concerning the origin of their polarity properties or γ^+ components. These polar probes are then utilized to determine the γ^{AB} contributions and an apolar probe liquid to determine γ^{LW} (21). Table I lists the properties of the probe liquids used in this study to determine θ on the film surfaces. In this study, contact angles values were included in 3 substituted expanded Young-Dupré equations and simultaneously solved. The apolar component was calculated from the reduced Young-Dupré equation (Eq. 2):

$$(1+cos\theta)\gamma_L = 2\left(\gamma_S^{LW}\gamma_L^{LW}\right)^{1/2} \quad (2)$$

Finally, the polar component (Lewis acid–base) was estimated from Eq. 3 after having determined the surface tension components of the solid surface:

$$\gamma^{AB} = 2\left(\gamma_S^{+}\gamma_S^{-}\right)^{1/2} \quad (3)$$

Fig. 2 SEM image of a ~400 μm-thick film which was loaded to contain ▶ 10% w/w DOXY. (**a**) depicts the smooth surface after 4 h exposure to the dissolution medium. (**b**) is a cross section of the film, showing the solid, impervious interior of the film. (**c**) indicates gradual erosion of the drug from the film surface after 72 h.

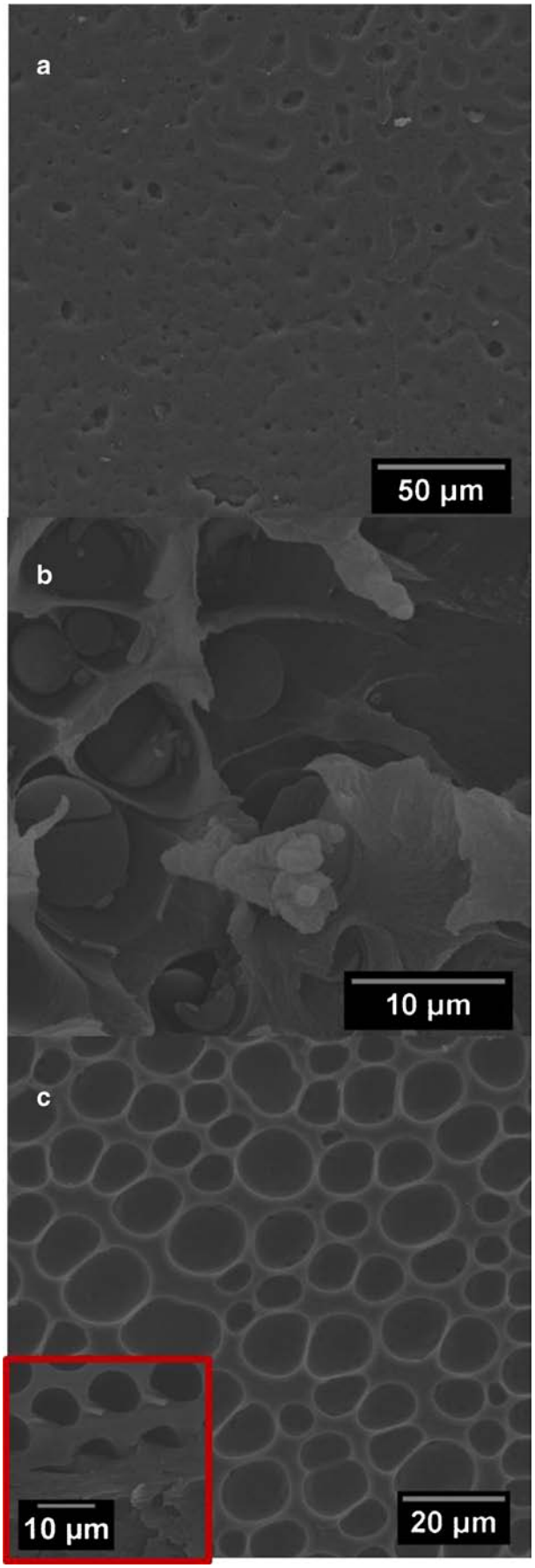

Fig. 3 SEM image of a ~400 μm-thick film which was loaded to contain 10% w/w CLR. (**a**) depicts the film surface after 4 h exposure to the dissolution medium with pores opening up. (**b**) is a cross section of the film, showing the honeycomb interior of the film containing the antibiotic. (**c**) indicates the surface the films after 72 h from which the drug was eroded from the surface cavities and therefore opening the pores reaching into the interior of the honeycomb structure.

The polarity of the solid is the ratio of γ_{AB} to γ (calculated using Eq. 4) expressed in percentage as $\%P$ in this report (22):

$$\gamma = \gamma^{LW} + \gamma^{AB} \tag{4}$$

Where the total surface tension of a component is given by γ, the apolar component of the surface tension or Lifshitz-van der Waals-components are given by γ^{LW} and the polar or Lewis acid–base contributions are given by the term, γ^{AB}.

To measure contact angles, droplets of the probe liquids of 10 μL were deposited on the samples and the contact angle was measured directly with a telescopic goniometer (Gaertner Scientific Corporation, Skokie, Illinois) at 23°C. Eight measurements were made on the prepared films to produce measurement errors smaller than 2° as is commonly found employing this technique (23).

Biofilm Reactor Studies

A drip flow biofilm reactor (BioSurfaces Technologies, Bozeman, MT) was employed to study biofilm formation on the polymer films (24). Control polymer films containing no antibiotics were used as reference ($n=3$). Antibiotic-loaded films ($n=3$) were used to investigate their effect on biofilm formation.

The biofilm is created by inoculating the drip flow reactor block with the test organism at an inoculum of 10^6 and incubating for 18–24 h at 37°C. The reactor block is angled at 10° to allow gravitational draining of the supplement media. A peristaltic pump delivers media to the reactor block to support biofilm growth. All biofilm growth and testing was performed with tryptic soy broth supplemented with 1% glucose to support biofilm growth. Two isolates were evaluated in the drip flow reactor: (1) *S. aureus* ATCC 29213 (MSSA) and (2) a clinical MRSA isolate recovered from a patient with a post-surgical device infection designated as strain 203. Changes in the log 10 CFU/ml after 48 h and 72 h compared to controls were evaluated for each drug/polymer film tested by analysis of variance with Tukey's post hoc test. A P value of$\leq$0.05 was considered significant. All statistical analyses were performed using SPSS statistical software (release 17.0; IBM Corporation, Armonk, New York).

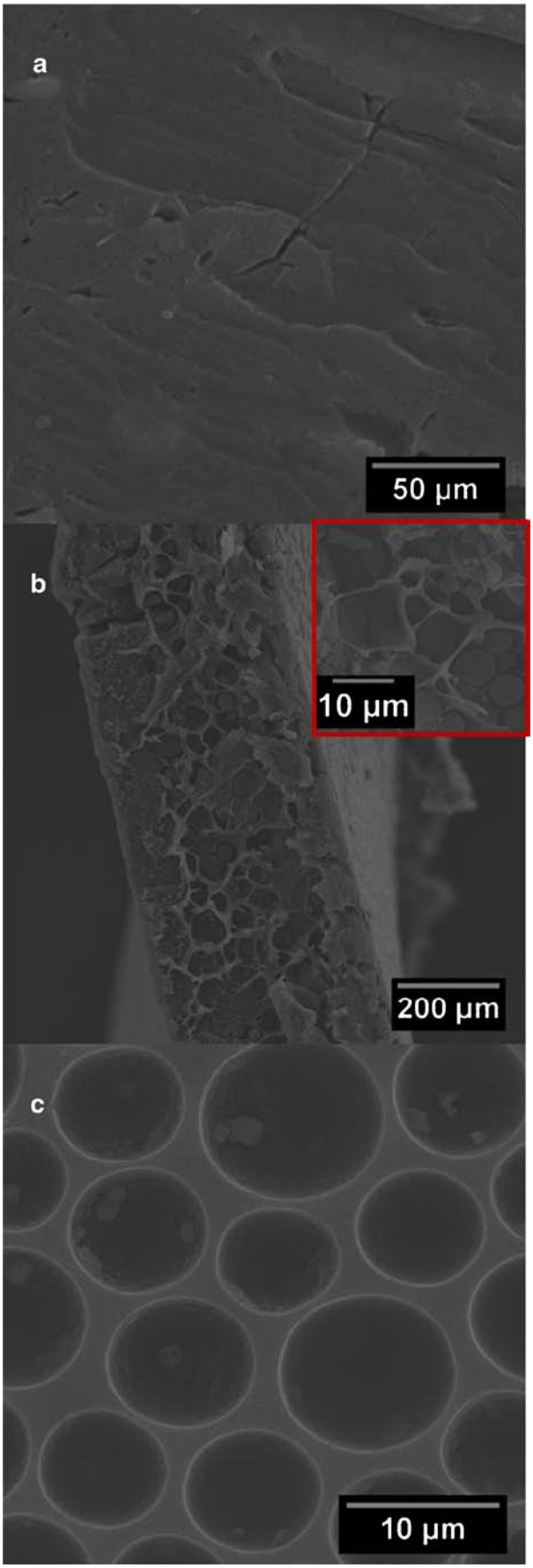

Fig. 4 SEM images of a ~400 μm thick film containing 10% RIF:DOX (1:1). ▶ (**a**) shows the film after 4 h in dissolution medium showing a relatively smooth surface. (**b**) cross-section close-up interior view of films showing honeycomb (insert) filled with RIF (red box). (**c**) shows a surface view of films after 72 h dissolution showing empty pockets with polymer scaffolding in place.

RESULTS AND DISCUSSION

Copolymerization

Table II summarizes the properties of the copolymers that were synthesized. High weight copolymers were synthesized and 3 were selected based on their suitability to form films (16). The film casting was found to be optimal when approximately 30% MMA was contained in the film.

Drug Release

The copolymer films that were produced showed a complex interior structure that formed due to coacervation. Figures 1, 2, 3, 4 and 5 shows the morphology of the antibiotic films before and after drug loading and release studies. Coacervation of the polymer-drug formulation resulted in the heavier molecular weight fraction of the polymer to precipitate as evaporation of the solvent took place followed by continuously lighter fractions. Subsequently, solvent-rich zones formed in the latex that was encapsulated by the precipitated polymeric material. On complete evaporation of the solvent, a honeycomb structure remained with the drug captured in various pockets of the film. Some of the drug escaped encapsulation and migrated to the surface as a pervaporation product. Two potential sources of drug release was thus formed i.e. a surface-deposited drug layer and the interiorly encapsulated drug (Fig. 6).

Antimicrobial Studies

The bioreactor studies complimented the observations made during the release studies and contact angle measurements (discussed later) by demonstrating significant inhibition of bacterial rebound at during the stated test period. An example of a continuous drip-flow bioreactor study is shown in Fig. 7. After a period of 72 h SEM analysis was again performed on the films to determine if bioadhesion took place. Figure 8 shows the SEM images that were recorded. As an indicator of the effect that the antimicrobial films had on the inoculum of the various microorganisms, biofilm density was measured over time. Figure 9 shows the results of biofilm density measurements.

The biofilm measurements showed that the control films were virtually ineffective at preventing biofilm formation. The

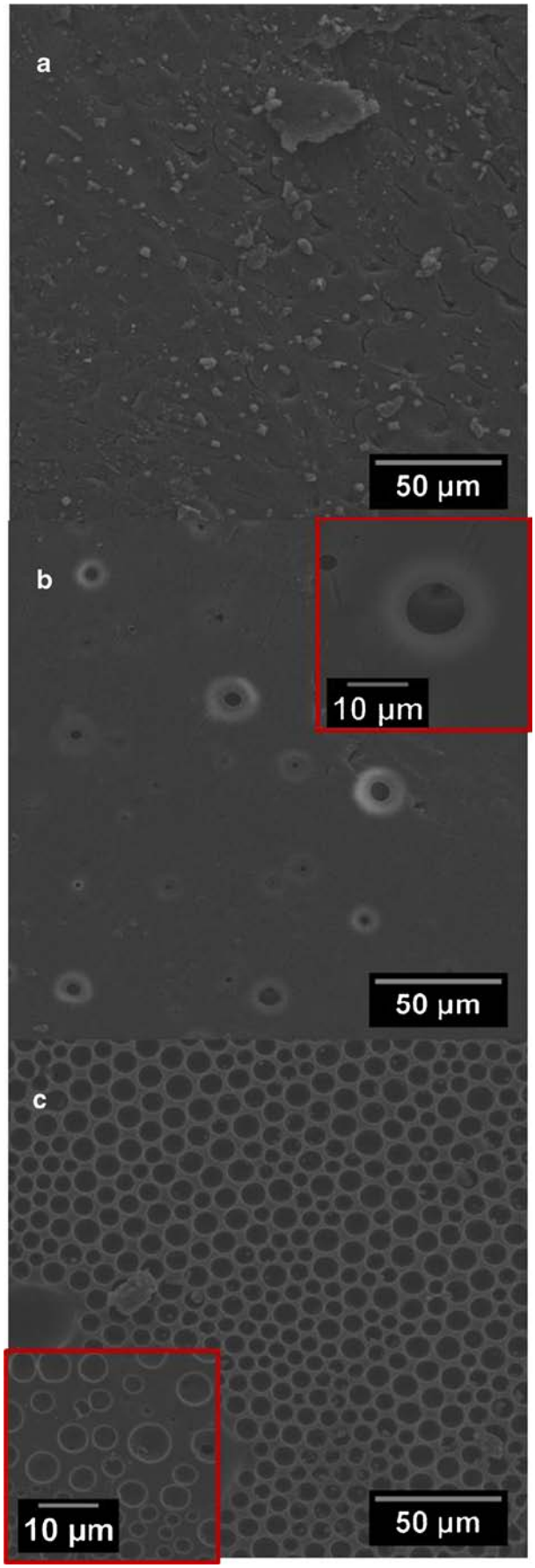

Fig. 5 SEM pictures of a ~400 μm thick film containing 10% RIF:CLR (1:1). (**a**) shows the film before dissolution medium showing a relatively smooth surface. (**b**) erosion of drug particles from the surface exposed drug-filled pockets that are connected to interior pockets (see insert). (**c**) shows a surface view of films after 72 h in dissolution medium showing empty pockets with polymer scaffolding in place.

films that contained only a single antibiotic were effective for a limited period of time before bacterial rebound of the film was observed. CLR proved most effective as a single antimicrobial during the 72 h period of incubation. Combinations of antibiotics proved superior in their prevention of biofilm formation, providing >99.9% kill of organisms at 48 h and 72 h from the initial inocula. The RIF-CLR combination was the most effective regimen tested. Additionally, this combination prevented rebound of the biofilm during the 48–72 h incubation period.

Contact Angle and Solid Surface Tension Components

To obtain some measure of the surface properties of the films and how it related to changes in drug release and biofilm formation contact angles were measured using DIM, water and EG. The results of the measurements for blank films and antibiotic-loaded films are reported in the supplementary information. Table III lists the average values of the surface tensions components that were calculated for the various films.

Measurements of the contact angles also demonstrated the changes that were seen in the relative surface tension components of the solid surface of the copolymer film as the drug eluted from the carrier. This was also suggested from preconditioning of metal surfaces with ferric ions or microorganisms to modify the physicochemical surface properties of the metal surfaces. Subsequently, adsorption of planktonic-form microorganisms could be controlled (25). The antibiotics were therefore, essential to eliminate the microorganisms since the empty surface cavities or drug-devoid copolymer control films would seem more favorable to facilitate the adsorption of bacteria to the copolymer film due to an increase in the hydrophobicity of the copolymer surface due to drug elution. Several contradictory results have been reported that state that hydrophobic surface will either increase or decrease adhesion of bacteria and that is mostly attributed to analysis of a single parameter whereas multiple factors indeed determine adhesion (26). Therefore, a case-by-case evaluation, of situations in which adhesion would take place *in vivo*, is justified.

In addition to the contact angle measurements made on films, compacted drug pellets were also evaluated using water to determine their contact angles. CLR showed a contact angle of 91±2.1°, RIF an angle of 83±2.3° and DOX an angle of 48±3.1°. This resulted in water-drug work of adhesion (W_A) values of ~71.1 mJ/m^2, ~81.2 mJ/m^2 and

120.8 mJ/m^2 for CLR, RIF and DOX respectively. Seen from the theoretical perspective of perfect wetting where $\theta \rightarrow 0°$, the maximum W_A is seen for water with a value of ~145 mJ/m^2, these pure drugs show their relative wettability in water and to their respective copolymer films preparations as shown in Table III. The W_A was higher for CLR was approximately 14% higher in the film compared to the free drug. RIF also demonstrated a significantly higher (~15.5%) W_A in the film. However, CL incurred a W_A penalty when formulated in a film of ~10.4%, indicating poorer wetting of the drug with poorer dissolution as illustrated in the previous section.

An immediate concern is the fact that θ was determined at 23°C and not 37°C as was encountered during the release studies. The γ^{LW} and γ^{AB} surface tension components were, however reported for DIM, water and EG at various temperatures (27). Based on these results, the γ^{LW} and γ^{AB} components of the probe liquids were calculated for the release medium conditions.

DIM had a γ^{LW} value of 50.4 mJ/m^2 at 23°C *versus* 48.3 mJ/m^2 at 37°C, a ~4% decrease. Similarly, for water the γ^{LW} value of 21.7 mJ/m^2 decreased by ~3% to 21.1 mJ/m^2. Lastly, EG demonstrated a ~2.4% decrease from an γ^{LW} value of 28.8 mJ/m^2 to 28.1 mJ/m^2. It is concluded that the apolar surface tension component of the probe liquid will thus act essentially the same at these temperatures.

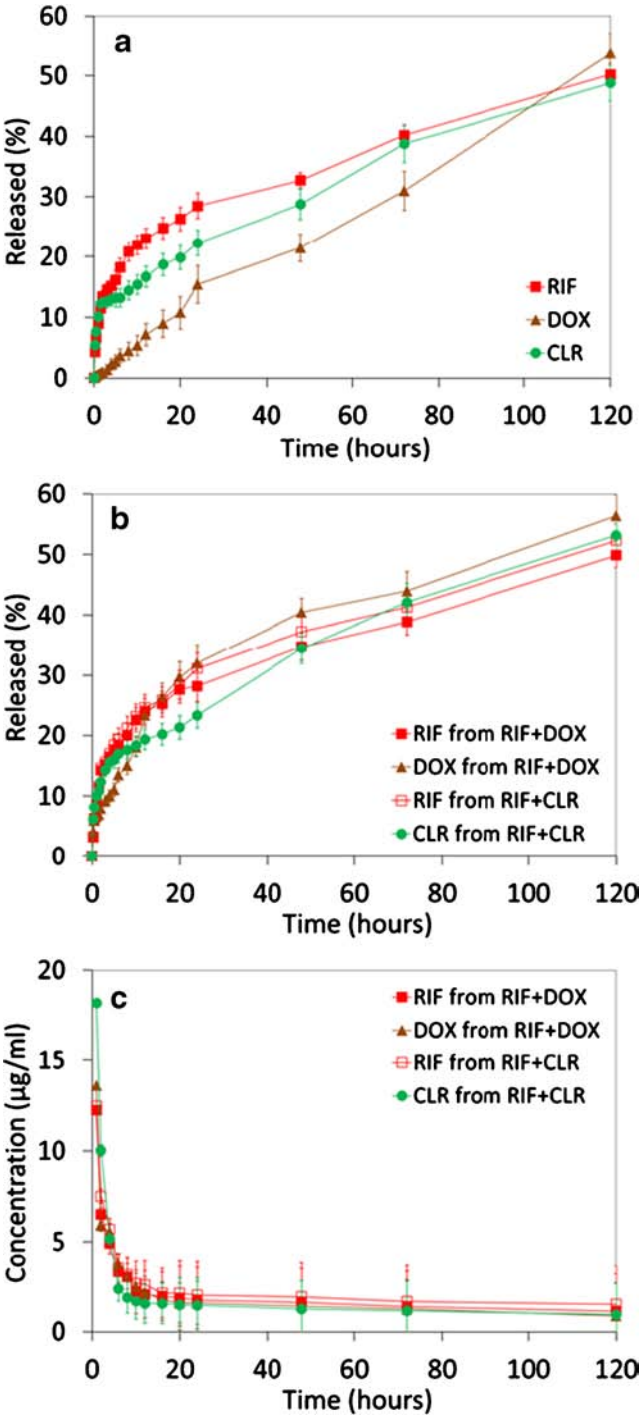

Fig. 6 The release of drugs from (**a**) singly loaded antibiotic and (**b**) combination of antibiotic-loaded films ($n = 6$). A faster release is observed during the first 20 h, followed by a slower, more sustained release phase up to 120 h. (**c**) The concentration of drug in the effluent produced in the bioreactor as a function of time. Results are shown only for the combination films because the release from single drug films was similar.

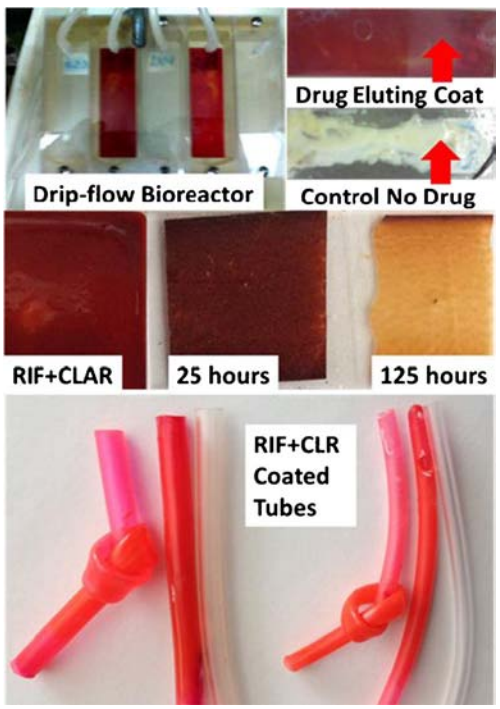

Fig. 7 At the top photographs of polymer coated glass slides in the bioreactor shown. The bioreactor shows control polymer films devoid of drug next to each rifampin-loaded film (red films) which showing drip sections where the antibiotic eluted. Next to it is a drug eluting coat devoid of biofilm and a control with biofilm formed. In the middle a RIF+CLR polymer coat is shown before being place in the dissolution vessels and after 25 and 125 h dissolution. The bottom photographs show different diameter uncoated nasogastric tubes and dip coated with the RIF+CLR polymer mixture. The flexibility of the coating is demonstrated by the knots tied in the tubes.

DISCUSSION

Drug Release

The copolymer films that were produced here are insoluble in aqueous media. They do however allow the loaded antibiotics to be released since diffusion of the release medium is possible through the porous interior of the film or by erosion of the drug from surface cavities. Our previous report (15) showed that the contact angle of the release medium with RIF films were significantly more favorable to interaction between the medium and the film surface with contact angles. After drug release, the contact angles were significantly altered to reflect poorer interaction between the PBS medium and film surface.

The films that captured a significant portion of the drugs in the surface cavities, therefore RIF (Figs. 1 and 4) and CLR (Figs. 3 and 5), showed a significantly faster drug release compared to the seemingly impervious DOX films. Figure 6(a and b) shows the release patterns of antibiotics from the films. RIF and CLR showed and initial burst release of about 10–20% of the drugs up to 2–5 h, followed by slower release up 20 h. This was followed by even slower, almost zero-order release, up to 120 h (time tested). Within the 120 h about 50% of the drugs were released from the films. The release of DOX showed no burst release in a single-drug film but did when combined with RIF. The results indicate that the surface-captured drugs were eroded during the initial release period and the drug molecules were significantly more accessible to the release medium molecules resulting in their dissolution. The medium could, however, also permeate the film interior to cause additional dissolution of the drug in the interior of the honeycomb film structure. This interior fraction can therefore also contribute to the overall release of the drug from the film. The initial faster release phase that took place during the first 20 h of release may, however, be due to the surface-captured drug and the slower, secondary phase, which demonstrated near zero-order release, can be attributed to the slower diffusion of the drug from the interior porous matrix structure. In addition the RIF release might have been impeded more significantly due to the molecular weight of copolymer M28 which was double that of M9 or M44.

The data in Fig. 6(a and b) was used to calculate zero order release rates for the time period between 20 and 120 h. These rates were then used to predict how long it would take to release 100% of the drugs from the films. This estimation showed that theoretically RIF, DOX and CLR release could be sustained for up to 21 days. Figure 6(c) shows the release of the different drugs in the bioreactor. There was not a significant difference in the release of the drug as detected in the effluent flowing over the slides coated with the polymer/drug films. In the bioreactor, faster initial release of the drugs was also followed by much slower release. From these release

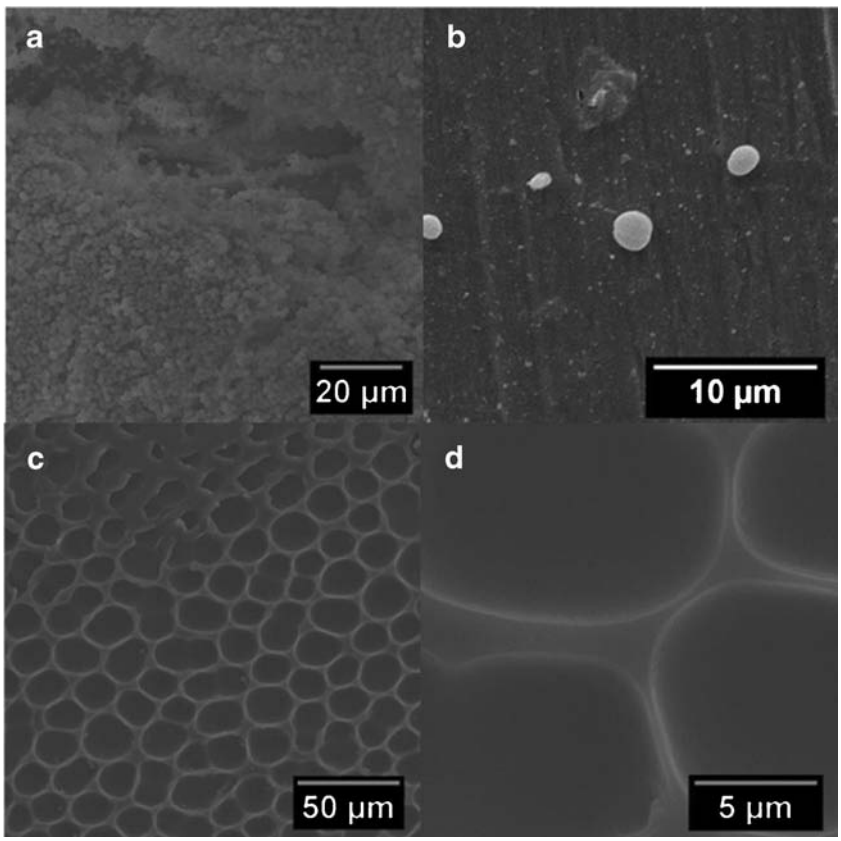

Fig. 8 Film samples taken from the bioreactor showing (**a**) the control film with abundant *S. aureus* biofilm growth, (**b**) a rifampin-loaded film sample after 24 h of incubation in the bioreactor showing a few cells, (**c** and **d**) shows sections of the surface of the films after 72 h incubation that were devoid of any biofilm formation.

profiles, a sustained release could be predicted for up to 21 days.

Biofilm Reactor

The drip flow bioreactor proved to be a useful technique to investigate both drug release and biofilm formation. Since the reactor was tilted at approximately 10° and subject to liquid flow, shear effects could also be illustrated. The copolymer films demonstrated their adhesion properties to both glass, which predominantly exposes silanol surface groups, and silicone tubing and resisted film coating detachment. Furthermore, antibiotic drug release could be observed over extended periods that indicated the dual functionality of the copolymeric material. Despite the failure of the control films to inhibit the growth of the pathogenic *S. aureus* species tested here, they effected a beneficial effect when loaded with antibiotics and favored the release of the drugs from the film. Subsequently, bacterial rebound was significantly prevented over sustained periods of time.

Contact Angle and Surface Tension Components

DIM has no polar component and γ^{AB} was calculated for water and EG. Water had a γ^{AB} value of 50.7 mJ/m2 at 23°C *versus* 49.1 mJ/m^2 37°C, a ~3% decrease at. EG showed a ~2.4% decrease from 18.9 mJ/m^2 to 18.4 mJ/m^2. It is concluded that the average values of the polar and apolar surface tension component of the probe liquid will thus change very little between these two temperatures. However, this can be misleading, because the constituent polar components for water (and other polar probe liquids), γ^+ and γ^- can change significantly from 20 to 38°C (28). Where the γ^+ and γ^- for water are both 25.5 mJ/m^2 at 20°C, they become 32.4 mJ/m^2 and 18.5 mJ/m^2 respectively at 38°C. At the release temperature of 37°C γ^+ becomes ~32.0 mJ/m^2 and γ^- becomes 18.9 mJ/m^2 implicating that water is a much stronger Lewis acid at the release temperature than at the contact angle measurement temperature and subsequently will lead to a marked reduction in the attractive energy between the polymer and water contact surface. Heating will thus have a strong effect on γ^+ of water and the interaction with electron donor compound such as poly(MMA) of which blocks may occur in the copolymers used here. Poly(S) also showed very strong hydrophobicity with a γ^{LW} of 42 mJ/m^2 with a γ^+ of 0 and γ^- of 1.1 mJ/m^2, the polar components being typically very low and close to zero (28).

From the values in Table III it is apparent that very complex interactions will take place between the release medium and the antibiotic-loaded copolymers films over time and also compared to the control films. Generally, all the film preparations showed significantly higher values for γ^- than for γ^+, the latter approaching zero. The relatively high values for γ^- is indicative of electron donor properties which would then require the appropriate electron accepting, γ^+, properties from the probe or "bacterial phase" for the Lewis acid–base pair interaction to take place. In PBS, however, several potassium cations are found and these neutralize and decrease γ^- of the surface to the point where the material will become hydrophobic (29).

Furthermore, most films showed a continuously decreasing polarity, γ^{AB}, from the loaded stage to the final stage at 80 h. The exception, however, is the M9 DOX film. It showed an increase in γ^{AB} with its γ^+ components increasing slightly over time in contrast to all other systems which showed a decrease in γ^+ components. Therefore, a slightly higher overall Lewis basicity evolved over time compared to the other film systems based on the ratio of γ^+ to γ^-. The Lewis acid water would thus have a much more favorable interaction with this film than the others and will cause a thicker stagnant water layer to slow down drug diffusion. Since the M9 DOX film also

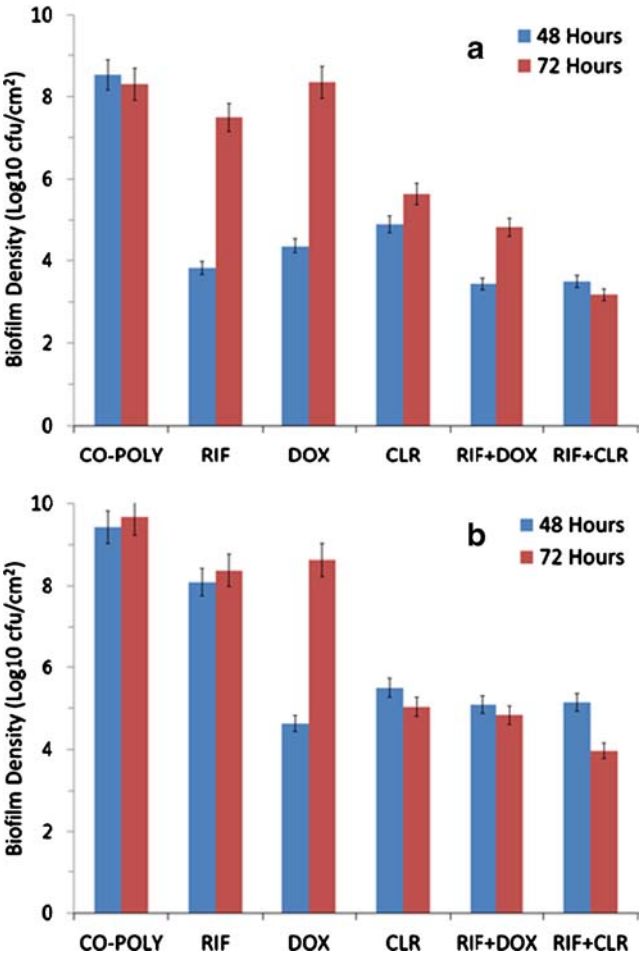

Fig. 9 Biofilm density was measured after 48 and 72 h to determine the efficiency of the antibiotic loaded films ($n = 3$) over time when tested in the bioreactor. (**a**) *S. aureus* ATCC 29213 (MSSA) and (**b**) *S. aureus* clinical isolate number 203 (MRSA). Biofilm density on all the drug eluting films were significantly less ($P \leq 0.05$) than controls after 48 h and for CLR, RIF+DOX and RIF+CLR even after 72 h.

Table III Calculated average γ component values of the copolymer films and W_A of the water-film interface (both in mJ/m^2) at 23°C ($n = 8$)

M9							
	γ_{LW}	γ^-	γ^+	γ_{AB}	γtotal	%P	W_A
Blank	44.42	0.598	0.002	0.061	44.48	0.1	69.35
DOX	42.53	27.15	0.147	3.993	46.52	8.6	108.2
25 h	41.40	21.65	0.219	4.357	45.75	9.5	101.1
80 h	38.40	17.95	0.281	4.493	42.90	10.5	94.10
M28							
	γ_{LW}	γ^-	γ^+	γ_{AB}	γtotal	%P	W_A
Blank	42.53	8.087	0.000	0.044	42.58	0.1	88.77
RIF	41.57	15.75	0.280	4.202	45.77	9.2	93.80
25 h	40.63	13.26	0.253	3.661	44.29	8.3	90.15
80 h	38.02	7.389	0.039	1.075	39.09	2.8	82.26
M44							
	γ_{LW}	γ^-	γ^+	γ_{AB}	γtotal	%P	W_A
Blank	43.24	4.280	0.005	0.282	43.52	0.7	81.01
CLR	43.34	5.997	0.155	1.926	45.27	4.3	81.48
25 h	42.03	2.014	0.022	0.422	42.45	1.0	75.97
80 h	40.69	0.678	0.040	0.330	41.02	0.8	69.66
M28:M44 (1:1)							
	γ_{LW}	γ^-	γ^+	γ_{AB}	γtotal	%P	W_A
Blank	42.20	5.351	0.000	0.057	42.25	0.1	83.51
RIF:CLR(1:1)	43.02	14.78	0.167	3.145	46.17	6.8	94.85
25 h	38.21	11.48	0.049	1.502	39.71	3.8	88.77
80 h	37.43	4.996	0.002	0.190	37.62	0.5	78.65
M28:M9 (1:1)							
	γ_{LW}	γ^-	γ^+	γ_{AB}	γtotal	%P	W_A
Blank	40.75	5.084	0.027	0.739	41.49	1.8	76.13
RIF:DOX(1:1)	41.63	9.579	0.003	0.318	41.95	0.8	90.15
25 h	40.75	5.084	0.027	0.739	41.49	1.8	80.06
80 h	37.89	2.549	0.000	0.050	37.94	0.1	72.98

showed the highest extent of biofilm rebound, the bacterial biofilm should also create a suitable Lewis acid character to facilitate its absorption.

The change to a more hydrophobic surface over time at least in part implies that the recovery of bacterial growth on the surface can be attributed to a hydrophobic attraction between the eventual biofilm and copolymer surface. This was seen for all the copolymer surfaces that showed a rebound in biofilm growth over time with the exception of the film preparation containing RIF:CLR (1:1) in the film containing M28:M9 (1:1). It would therefore, be apparent that it is imperative to include the antibiotics in the combinations to eradicate the biofilm without subsequent recurrence of growth. The fact that CLR:RIF (1:1) performed the best in the biofilm studies could be ascribed to their W_A values which indicated superior wetting properties in the medium compared to the RIF:DOX (1:1) which showed higher W_A values. This implies that contact between CLR:RIF combination and release medium was higher than for other film preparations. Therefore a thicker stagnant layer (release medium) could be present on the polymer film surface than for the other combinations. This reduced the release rate of the CLR:RIF over time compared to the other combinations. Therefore, drug could be released over a longer period of time from this combination than from the other combinations. The fact that the combinations of antibiotics outperformed the single drug films, indicated the efficiency and need for combination therapy since multidrug resistance is a known problem.

CONCLUSION

More than 99% of all microorganisms in nature will be found in the form of biofilms. In clinical infections, the National Institutes of Health estimates that biofilms contribute to 80% of microbial infections in the body. Certain types of biofilms have evolved to be multidrug resistant. In the hospital setting where invasive procedures such as surgery, intubation, implantation and prolonged exposure to disease environments are encountered, these biofilms flourish. It is of utmost importance

to prevent the formation of these biofilms, since hospital-acquired infections are some of the toughest and often fatal infections to treat.

In this study we report the effect of single and combinations of antibiotics formulated in poly(S-*co*-MMA) films where the combinations of antibiotics proved most effective in biofilm rebound prevention by MSSA and MRSA. The copolymeric films showed very good adhesion to glass and silicone tubing, two common materials in the biomedical environment. Additionally, the dual functionality of the copolymer coating could be illustrated by its extended drug release properties that successfully curbed pathogenic rebound on the film surfaces. The film surfaces were characterized according to their surface tension components and it was found that the films generally become more hydrophobic over time as the antibiotic elutes from the film. Since many microorganisms are prone to attachment to hydrophobic surfaces according to the Lifshitz-van der Waals theory, it is imperative to add antibiotics to eradicate biofilms from surfaces where they could potentially adhere and proliferate.

Future studies should be undertaken to use the surface tension component approach in combination with surface profilometry and additional drug/adjuvant combinations to design appropriate materials or drug-loaded film delivery systems to ensure biofilm prophylaxis of other infections. More work is also needed to determine the applicability of the poly(S-*co*-MMA) films to coat implantable devices. In Fig. 7 nasogastric tubes coated with the films are shown. This preliminary example shows the potential and flexibility of the combination drug films tested in this study.

REFERENCES

1. Costerton JW, Stewart PS, Greenberg EP. Bacterial biofilms: a common cause of persistent infections. Science. 1999;284(5418): 1318–22.
2. Veesenmeyer JL, Hauser AR, Lisboa T, Rello J. *Pseudomonas aeruginosa* virulence and therapy: evolving translational strategies. Crit Care Med. 2009;37(5):1777–86.
3. Donlan RM. Role of biofilms in antimicrobial resistance. ASAIO J. 2001;46(6):S47–52.
4. Gordon CA, Hodges NA, Marriott C. Antibiotic interaction and diffusion through alginate and exopolysaccharide of cystic fibrosis-derived *Pseudomonas aeruginosa* with piperacillin and tobramycin. J Antimicrob Chemother. 1988;22(5):667–74.
5. Donlan RM, Costerton JW. Biofilms: survival mechanisms of clinically relevant microorganisms. Clin Microbiol Rev. 2002;15(2):167–93.
6. Prabhakara R, Harro JM, Leid JG, Keegan AD, Prior ML, Shirtliff ME. Suppression of the inflammatory immune response prevents the development of chronic biofilm infection due to methicillin-resistant *Staphylococcus aureus*. Infect Immun. 2011;79(12): 5010–8.
7. Darouiche R. Device-associated infections: a macroproblem that starts with microadherence. Clin Infect Dis. 2001;33(9):1567–72.
8. Raad I, Costerton JW, Sabharwal U, Sacilowski M, Anaissie E, Bodey GP. Ultrastructural analysis of indwelling vascular catheters: a quantitative relationship between luminal colonization and duration of placement. J Infect Dis. 1993;168(2):400–7.
9. Stoodley P, Ehrlich GD, Sedghizadeh PP, Hall-Stoodley L, Baratz ME, Altman DT, *et al.* Orthopaedic biofilm infections. Curr Orthop Pract. 2011;22(6):558–63.
10. Esfandiari N, Simchi A, Bagheri R. Size tuning of Ag-decorated TiO_2 nanotube arrays for improved bactericidal capacity of orthopedic implants. J Biomed Mater Res A. (2013):In press.
11. Strydom SJ, Rose WE, Otto DP, Liebenberg W, de Villiers MM. Poly(amidoamine) dendrimer-mediated synthesis and stabilization of silver sulfonamide nanoparticles with increased antibacterial activity. Nanomedicine Nanotechnol Biol Med. 2013;9(1):85–93.
12. Tan H, Ma R, Lin C, Liu Z, Tang T. Quaternized chitosan as an antimicrobial agent: antimicrobial activity, mechanism of action and biomedical applications in orthopedics. Int J Mol Sci. 2013;14(1): 1854–69.
13. Janjaroen D, Ling F, Monroy G, Derlon N, Mogenroth E, Boppart SA, *et al.* Roles of ionic strength and biofilm roughness on adhesion kinetics of *Escherichia coli* onto groundwater biofilm grown on PVC surfaces. Water Res. 2013;47(7):2531–42.
14. Lichter JA, Thompson MT, Delgadillo M, Nishikawa T, Rubner MF, van Vliet KJ. Substrata mechanical stiffness can regulate adhesion of viable bacteria. Biomacromolecules. 2008;9(6): 1571–8.
15. Otto DP, Vosloo HCM, Liebenberg W, de Villiers MM. Effects of the cosurfactant 1-butanol and feed composition on nanoparticle properties produced by microemulsion copolymerization of styrene and methyl methacrylate. J Appl Polym Sci. 2008;107(6):3950–62.
16. Otto DP, Vosloo HCM, Liebenberg W, de Villiers MM. Development of microporous drug-releasing films cast from artificial nanosized latexes of poly(styrene-*co*-methyl methacrylate) or poly(-styrene-*co*-ethyl methacrylate). Eur J Pharm Biopharm. 2008;69(3): 1121–34.
17. USP. United States Pharmacopeia (USP-36-NF 31). The United States Pharmacopeial Convention, Rockville; 2014.
18. De Villiers MM. Anti-tuberculosis drugs. In: Cazes J, editor. Encyclopedia of chromatography, vol. 1. 3rd ed. Boca Raton: CRC Press; 2010. p. 118–23.
19. Balkende AR, van de Boogaard HJAP, Scholten M, Willard NP. Evaluation of different approaches to assess the surface tension of low-energy solids by means of contact angle measurements. Langmuir. 1998;14(20):5907–12.
20. Van Oss CJ, Good RJ, Chaudhury MK. Additive and nonadditive surface tension components and the interpretation of contact angles. Langmuir. 1988;4(4):884–91.
21. Van Oss CJ. Use of the combined Lifshitz-van der Waals and Lewis acid–base approaches in determining the apolar and polar contributions to surface and interfacial tensions and free energies. J Adhes Sci Technol. 2002;16(6):669–77.
22. Van Oss CJ, Good RJ. Prediction of the solubility of polar polymers by means of interfacial tension combining rules. Langmuir. 1992;8(12):2877–9.
23. Lam CNC, Lu JJ, Neumann AW. Measuring contact angle. In: Holmberg K, editor. Handbook of applied surface and colloid chemistry, vol. 2. Chichester: John Wiley & Sons; 2002. p. 251–80.

24. Agostinho AM, Hartman A, Lipp C, Parker AE, Stewart PS, James GA. An in vitro model for the growth and analysis of chronic wound MRSA biofilms. J Appl Microbiol. 2011;111(5): 1275–82.
25. Briandet R, Herry JM, Bellon-Fontaine MN. etermination of the van der Waals, electron donor and electron acceptor surface tension components of static Gram-positive microbial biofilms. Coll Surf B. 2001;21(4):299–310.
26. Desrousseaux C, Sautou V, Descamps S, Traoré O. Modification of the surfaces of medical devices to prevent microbial adhesion and biofilm formation. J Hosp Infect. 2013;85(2):87–93.
27. Fan CW, Lee SC. Surface free energy effects in sputter-deposited WN_x films. Mater Trans. 2007;48(9):2449–53.
28. Van Oss CJ. Hydrophobicity of biosurfaces – origin, quantitative determination and interaction energies. Coll Surf B. 1995;5(3–4):91–110.
29. Van Oss CJ. Interfacial forces in aqueous media. FL:CRC Press; 2006.